Research Article

iMedPub Journals
http://www.imedpub.com

Chemical biology and Pharmaceutical chemistry

2020
Vol. 3 No. 3

DOI: 10.36648/J Chem Biol Pharm Chem.3.3.133

In silico Analysis of Structure Activity Relationship of ω-Conotoxins with Cav 2.2 Channel Receptor for Treatment of Neuropathic Pain

Muhammad Sibte Hasan Mahmood , Tiyyaba Furqan[2], Sidra Batool[2*]

[1]Grand River Hospital, Medicine Department, 835 King St W, Kitchener, ON N2G 1G3, Canada

[2]Department of Biosciences, COMSATS University, Park Road, Chak Shahzad, Islamabad, 45550, Pakistan

Corresponding author: Sidra Batool

Department of Biosciences, COMSATS University, Park Road, Chak Shahzad, Islamabad, 45550, Pakistan

sidra.batool@comsats.edu.pk

Citation: Batool S (2020) In silico Analysis of Structure Activity Relationship of ω-Conotoxins with Cav 2.2 Channel Receptor for Treatment of Neuropathic Pain. J Chem Bio Pha Chem Vol.3 No.3: 75

Abstract

Background: The N-type voltage-gated Ca2+ channel Cav2.2 is expressed predominantly at presynaptic neuronal terminals. They are predominantly expressed in nerve terminals, where they control neurotransmitter release. Also, this receptor transduces electrical activity into other cellular functions and plays an important role in processing pain information in nociceptive pathways.

Objective: To date, genetic and pharmacological studies have identified that high threshold, Cav 2.2 channel receptor is important for pain sensation in disease models. This suggests that Cav 2.2 channel receptor inhibitors or modulators could be developed into useful drugs to treat neuropathic pain.

Method: Many peptides are reported as potent and highly selective blockers of calcium channel function. Among them, cone snails are rich sources of such peptides and constitute class of conotoxins.

Results: In this study, structural and binding analysis of ω-conotoxins class have been done against Cav 2.2 channel receptor to investigate their role as therapeutic agents and analgesics.

Conclusions: Computational analysis revealed that certain structural motifs, in particular the inhibitor cysteine knot, prove to be quite common and play an important role in stability and inhibition of Cav2.2 along with certain other residues amongst this class of peptides.

Keywords: In silico; Cav 2.2 channel receptor; ω-conotoxins; Neuropathic pain; Transmembrane helices.

Received: October 01, 2020; **Accepted:** October 22, 2020
Published: October 30, 2020

Introduction

'T'Voltage gated calcium channels (VGCCs) mediate a number of neuronal functions including neurotransmitter release, neuronal excitation, neurite outgrowth and regulation of gene expression. VGCCs have a molecular complex comprised of several subunits that consists of α1, α2-δ, β and ɤ (Figure 1a) [1]. The α1 subunit is essential for channel functioning and determines fundamental channel properties. The pore forming transmembrane α1 subunit is organized in four homologous domains (I-IV) [1], comprising six transmembrane α helices (S1-S6) and the pore forming P loop between S5 and S6 (Figure 1b) [2]. Gene encoding 10 pore-forming α1 as well as several splice variants have been identified and characterized. Neuronal VGCCs include Cav 1.1 and Cav 2.2 channels have predominantly expressions at presynaptic neuronal terminals throughout the central nervous system [3]. They are involved in supplying the signal Ca(2+) important for the sustained neuronal firing and neurotransmitter release characteristics of different syndromes including neuropathic pain, abnormal and pathological responses that develop as a consequence of injury. There are number of reported studies that use calcium channels as receptor against neurodegenerative disorders [4,5]. Among them, Cav2.2 is a calcium channel subtype localized at nerve terminals, including nociceptive fibers, where it initiates neurotransmitter release. Cav2.2 is an important contributor to synaptic transmission in ascending pain pathways

and is up-regulated in the spinal cord in chronic pain states along with the auxiliary α2δ1 subunit. It is therefore not surprising that toxins that inhibit Cav2.2 are analgesic. Preclinical data have identified Cav 2.2 as key participant in contributing to these Ca(2+) signaling events. There are several therapeutic strategies for treatment of neuropathic pain [6–8]. Clinical data with the peptide blocker Prialt also validated Cav 2.2 as a bona fide target for drug discovery efforts to identify new and novel therapeutics for neuropathic pain [9].

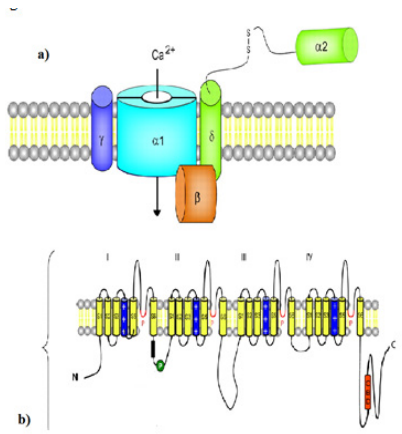

Figure 1 Predicted membrane topology, subunit interactions and structural domains of the auxiliary subunits of voltage-gated calcium channels, (a) The voltage-gated calcium channels are composed of the pore forming α1 subunit and the auxiliary α2δ, β and ɤ subunits, (b) α1 subunit is composed of four domains (I-IV), comprising six transmembrane helices (S1-S6) and the extracellular P loop between S5 and S6 (Hofmann et al., 1999).

A wide diversity of venomous animals has evolved a large range of peptide toxins that target ion channels expressed in the neuronal and neuromuscular systems of prey and predators as part of efficient pre immobilization and deterrent strategies [10]. Many peptides are potent and highly selective blockers or modulators of calcium channel functions, and as such are valuable pharmacological tools and potentially valuable leads for the development of human therapeutics. Cone shells and spiders are rich sources of remarkably potent and selective Cav2.2 inhibitors.[11,12] The objective of this study was to perform the in silico analysis of binding interaction of ω-Conotoxins with the Cav 2.2 channel receptor. This class of conotoxins are reported to block calcium channels particularly Cav2.2 channel. This study is designed to computationally analyze the interactions of ω-conotoxins with Cav2.2 calcium channel. The mode of interaction and the binding residues for both the ligand dataset and receptor were collected. Due to unavailability of the crystal structure of Cav 2.2 channel receptor in humans and most of the conotoxins too, the 3D structures were predicted computationally. The analysis of the binding interactions of the receptor and the ligand peptides can help to demonstrate the pharmacological importance of the conotoxins and their potential use as Cav 2.2 channel receptor antagonists for treatment of neuropathic pain [13].

Materials and Methods

Receptor Collection

The 3D structure of Cav 2.2 channel receptor in human was predicted computationally using I-TASSER [14]. It allows automatic generation of high-quality predictions of 3D structure of protein molecules from their amino acid sequences. It is reported that Cav 2.2 plays an important role in neuronal communication and neurotransmitter release. Thus, they are molecular targets for pharmacological agents as well as for broad range of potent neurotoxins. Cav 2.2 channels are reported as main target of ω-conotoxins [1]. The α1 subunit of Cav 2.2 channel receptor is essential for channel functioning and determines fundamental channel properties. Domain III region of α1 subunit of Cav 2.2 channel receptor is the molecular target for broad range of venom toxins. These toxins act on region between S5 and S6 helices of domain III. These toxins physically block the pore of receptor. The binding site of these toxins has been mapped primarily to the external vestibule of the channel in the domain III pore-forming S5-S6 region [15]. In particular, residues Glu1326, Gln1327, Glu1332, Glu1334, Glu1337 and Gln1339 [16,17] were identified as being important for blockage by ω-conotoxins (Table 1).

Table 1: ω-conotoxins binding site on Cav 2.2 channel.

Receptor	Ligand	Receptor residues	Domain	Transmembrane region
Ca_v 2.2	ω-conotoxins	Gly1326, Gln1327, Glu1332, Glu1334, Glu1337, Glu1339	Domain III	Extracellular P loop

Ligand Dataset Collection

It is reported that a range of disulfide rich peptides from cone snails (conotoxins) preferentially inhibit Cav2.2. GVIA from Conus geographus has been used for many years as probe to discriminate Cav2.2 from other closely related Cav channel subtypes. In addition, several cone snail toxins have direct diagnostic and therapeutic potential. A synthetic version of a Cav2.2 channel blocker toxin ω-conotoxin MVIIA (ziconotide, Prialt®), from the venom of the cone snail Conus magus is currently in use clinically, validating Cav2.2 as an analgesic target in humans [14].

As ω-conotoxins have surfaced their potential as modulators of Cav2.2 channel. So, in this study a data set of 16 different ω-conotoxins was taken to study binding interactions with the Cav 2.2 channel receptor computationally [18] (Table 2). They are generally small, 10-30 amino acids, and rich in disulfide bonds, often containing unusual post-translationally modified amino acids [19]. ω-conotoxins are classified into three structurally different classes on the basis of characteristic arrangement of cysteine residues. The presence of a 'disulfide through disulfide knot' structurally defines these peptides as a "Knottin" [20]. This order of cysteine framework (C-C-CC-C-C) is highlighted in red color in Table 2. These six conserved cysteine residues are important for the maintenance of the tertiary structure of the conotoxins. The known structures of ω-conotoxins on Protein databank were only of three conotoxins, i) GVIA, ii) MVIIA and iii) MVIIC. Their PDB ids are 1TTL, 1TTK and 1CNN respectively.

The 3D structures of rest of the ω-conotoxins (CnVIIA, CVIA, CVIB, CVIC, CVID, CVIE, CVIF, FVIA, GVIB, GVIIA, GVIIB, RVIA and TVIA) were not available on the Protein data bank [21], therefore the structures were predicted computationally using I-TASSER [14]. A multiple sequence alignment (MSA) [22] was also performed on all the ω-conotoxins (Figure 2). It was observed that position 2 is occupied by lysine (K) and almost all the ω-conotoxins have a tyrosine (Y) residue at position 13 (Figure 2) [23, 24]. The binding determinants for the high affinity interaction of ω-conotoxins with Cav 2.2 channel have been proposed to rely on a two-point pharmacophore formed by the highly conserved tyrosine (Y13) and lysine (K2) [25, 26].

Table 2: Venom toxins selected as ligand data set, along with their amino acid sequence.

Venom toxin	Organisms of origin	Cysteine framework
ω-conotoxin CnVIIA	Cone snail	CKGKGAPCTRLMYDCCHGSCSSSKGRC
ω-conotoxin CVIA	Cone snail	CKSTGASCRRTSYDCCTGSCRSGRC
ω-conotoxin CVIB	Cone snail	CKGKGASCRKTMYDCCRGSCRSGRC
ω-conotoxin CVIC	Cone snail	CKGKGQSCSKLMYDCCTGSCSRRGKC
ω-conotoxin CVID	Cone snail	CKSKGAKCSKLMYDCCSGSCSGTVGRC
ω-conotoxin CVIE	Cone snail	CKGKGASCRRTSYDCCTGSCRSGRC
ω-conotoxin CVIF	Cone snail	CKGKGASCRRTSYDCCTGSCRLGRC
ω-conotoxin FVIA	Cone snail	CKGTGKSCSPRIAYNCCTGSCRSGKC
ω-conotoxin GVIA	Cone snail	CKSPGSSCSTSYNCCRSCNPYTKRCY
ω-conotoxin GVIB	Cone snail	CKSPGSSCSPTSYNCCRSCNPYTKRCYG
ω-conotoxin GVIIA	Cone snail	CKSPGTPCSRGMRDCCTSCLLYSNKCRRY
ω-conotoxin GVIIB	Cone snail	CKSPGTPCSRGMRDCCTSCLSYSNKCRRY
ω-conotoxin MVIIA	Cone snail	CKGKGAKCSRLMYDCCTGSCRSGKC
ω-conotoxin MVIIC	Cone snail	CKGKGAPCRKTMYDCCSGSCGRRGKCX
ω-conotoxin RVIA	Cone snail	CKPPGSPCRVSSYNCCSSCKSYNKKCG
ω-conotoxin TVIA	Cone snail	CLSXGSSCSXTSYNCCRSCNXYSRKCR

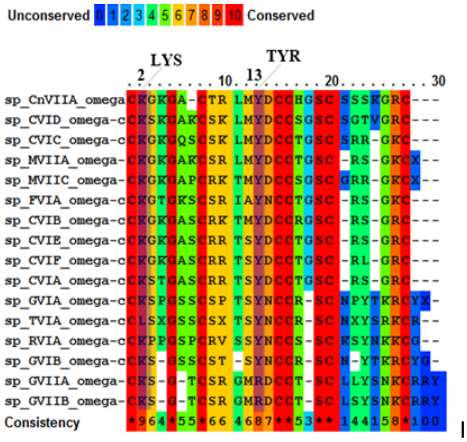

Figure 2 Multiple sequence alignment of ω-conotoxins. Two active residues, LYS at position 2 and TYR at position 13 have binding affinity for Cav 2.2 channel receptor in human are highlighted.

Docking Studies

Molecular docking is an important approach to evaluate the intercalation between potential ligands and their macromolecule targets. It also provides insights for identifying drug candidates and for designing novel or more effective drugs. To predict the binding mode of each venom ligands with the Cav 2.2 channel receptor, the docking studies were performed using AutoDock 4.2 [27]. The number of total docking runs were set to 50, which means that the receptor-ligand complexes were formed in 50 different conformations allowing the ligand to freely bind anywhere on the receptor for each conformation and then rank each conformation according to their stability. The grid size was set to cover the entire receptor in order to find a potential binding site for each ligand. The docking parameters used are shown in Table 3.

Table 3: Docking parameters used for docking studies on AutoDock 4.2.

Grid parameters		Docking parameters	
Spacing	0.375Å	Energy evaluations	2.5×10^6
Grid Center	80X Å	Iterations	27000
	80Y Å	Mutation rate	0.02
	80Z Å	Crossover rate	0.80
		Elitism value	1
		RMS tolerance	1.0 Å

The docking results were analyzed on AutoDock 4.2 and later visualized on Chimera [28]. Ligplot+ [29] was used to verify protein-protein interactions, which makes 2D schematics on the basis of hydrogen bonds and hydrophobic interactions. The 3D structural analysis was performed on Chimera that allowed the residues in the protein-protein interaction of the receptor-ligand complex to be highlighted. Based on the respective energy values achieved through dockings, the receptor-ligand binding was confirmed and refined which were then used for analysis and discussions of results.

Results

Prediction of the Structure of Cav 2.2 Channel in Humans

Full length structure of Cav 2.2 channel receptor in human was not available therefore the sequence of Cav 2.2 channel receptor was taken from UniProt to predict its 3D structure. This receptor contains four domains (I-IV). Each domain further contains six different transmembrane helices (S1-S6), and a extracellular P loop between S5 and S6 region. Residue range for transmembrane helix of each domain and extracellular P loop between S5 and S6 helices is mentioned in Table 4.

Table 4: Residue range for 6-helices of each domain along with extracellular P loop residue range.

Domains	Transmembrane helix	Amino acid range
Domain I (82-357)	S1	96-114
	S2	113-152
	S3	164-183
	S4	188-206
	S5	226-245
	S6	332-356
	P loop between S5 –S6	246-331
Domain II (468-712)	S1	483-501
	S2	517-536
	S3	545-564
	S4	574-592
	S5	612-631
	S6	685-709
	P loop between S5 –S6	632-684
Domain III (1137-1419)	S1	1152-1169
	S2	1186-1205
	S3	1218-1236
	S4	1247-1265
	S5	1285-1304
	S6	1392-1416
	P loop between S5 –S6	1305-1391
Domain IV (1456-1711)	S1	1472-1490
	S2	1506-1525
	S3	1534-1552
	S4	1564-1582
	S5	1602-1621
	S6	1684-1708
	P loop between S5 –S6	1622-1683

Figure 3 shows the linear sequence of Cav 2.2 channel receptor. This linear sequence is shown in four different color blocks. The predicted 3D structure of Cav 2.2 channel receptor is shown in (Figure 4). Four different domains (I-IV) of this receptor are shown in different colours. As each domain has bundle of six transmembrane helices (S1-S6). These transmembrane helices are reported as molecular targets for many peptides that alter the function of Cav 2.2 channel receptor. In Figure 4b, 3D structure of domain I is shown highlighting each transmembrane helices (S1-S6). The extracellular P loop is present between S5 and S6 region. Likewise in Figure 4c, 4d, 4e, 3D structures of each transmembrane helices (S1-S6) of domain II, domain III and domain IV are shown. The extracellular P loop which is present between S5 and S6 region is also highlighted for each domain.

Figure 3 Linear sequence of Cav 2.2 channel receptor with domains (I-IV) is shown in four different color blocks, (a) Sequence of Domain I in block of Tan color, containing sequence of each transmembrane helices (S1-S6) along with extracellular P loop, (b) Sequence of Domain II in block of light green color, containing sequence of each transmembrane helices (S1-S6) along with extracellular P loop, (c) Sequence of Domain III in block of Rosy brown color, containing sequence of each transmembrane helices (S1-S6) along with extracellular P loop, (d) Sequence of Domain IV in block of light purple color, containing sequence of each transmembrane helices (S1-S6) along with extracellular P loop.

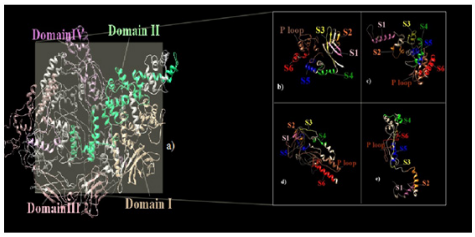

Figure 4 3D structure of Cav 2.2 channel receptor along with 4 different domains, Domain I is highlighted with Tan color, Domain II is highlighted with light green color, Domain III is highlighted with rosy brown color, Domain IV is highlighted with light purple color, b) 3D structure of each transmembrane helices (S1-S6) of Domain I are shown in different color, SI in hot pink , S2 in orange, S3 in yellow, S4 in green , S5 in blue and S6 in red color whereas extracellular P loop between S5 and S6 is highlighted with brown color, c) 3D structure of each transmembrane helices (S1-S6) of Domain II are shown in different color, SI in hot pink , S2 in orange, S3 in yellow, S4 in green, S5 in blue and S6 in red color whereas extracellular P loop between S5 and S6 is highlighted with brown color, d) 3D structure of each transmembrane helices (S1-S6) of Domain III are shown in different color, SI in hot pink , S2 in orange, S3 in yellow, S4 in green , S5 in blue and S6 in red color whereas extracellular P loop between S5 and S6 is highlighted with brown color, e) 3D structure of each transmembrane helices (S1-S6) of Domain IV are shown in different color, SI in hot pink , S2 in orange, S3 in yellow, S4 in green, S5 in blue and S6 in red color whereas extracellular P loop between S5 and S6 is highlighted with brown color.

3D Structure Prediction of ω-Conotoxins

3D structures of ω-conotoxins that are reported on PDB in addition with the predicted ones are represented in Figure 5.

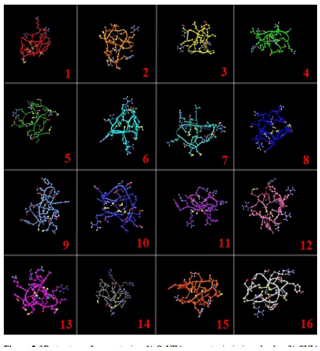

Figure 5 3D structure of ω-conotoxins: 1) CnVIIA ω-conotoxinsin in red color, 2) CVIA ω-conotoxins in orange color, 3) CVIB ω-conotoxins in yellow color, 4) CVIC ω-conotoxins in green color, 5) CVID ω-conotoxins in dark-green color, 6) CVIE ω-conotoxins in cyan color, 7) CVIF ω-conotoxins in light-sea green color, 8) FVIA ω-conotoxins in blue color, 9) GVIA ω-conotoxins comfort-blue color, 10) GVIB ω-conotoxins medium-blue color, 11) GVIIA ω-conotoxins in purple color, 12) GVIIB ω-conotoxins in hot-pink color, 13) MVIIA ω-conotoxins in magenta color, 14) MVIIC ω-conotoxins in dim-gray color, 15) RVIA ω-conotoxins in orange-red color, 16) TVIA ω-conotoxins in gary color..

Docking Results

After molecular docking of each venom ligands with Cav 2.2 channel receptor, docking results were run based on their energy values and ranked with each run showing results for receptor-ligand complex with the least energy. Detailed analysis of each run for each complex showed that all the ω-conotoxins showed binding interactions with the conserved active sites of Cav 2.2 channel in human. Almost all ω-conotoxins showed binding affinity with the residue GLY1326 and GLN1327 in the domain III region of Cav 2.2 channel (Table 5). Each complex was then further analyzed on Ligplot+ to identify the residues involved in the interaction between each ligand and the receptor. Table 5 contains the information about respective hydrogen bonds residues of both receptor and ligands, their hydrophobic residues, their bond distances and bond atoms. The complexes were further analyzed on Chimera [22] to find out the location of binding pocket of each venom ligand with the receptor molecule. It was observed that almost all venom ligands have same conserved binding pockets on receptor. Figure 6 shows that GLY at position 1326 and GLN at position 1327 were predominantly involved in the binding of α subunit of Cav 2.2 channel receptor in human with almost all the ω-conotoxins. The binding pattern of all the ω-conotoxin ligands individually in complex with the α subunit of Cav 2.2 channel receptor in human are shown in Figure 6.

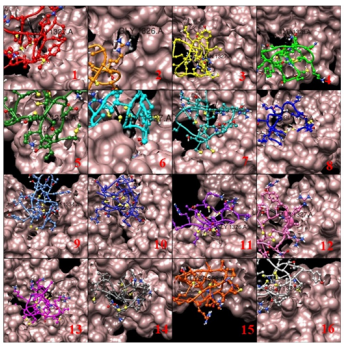

Figure 6 3D binding representation of Cav 2.2 channel receptor with each ω-conotoxin ligand. 1) ω-conotoxin CnVIIA in red color. 2) ω-conotoxin CVIA in orange color. 3) ω-conotoxin CVIB in yellow color. 4) ω-conotoxin CVIC in green color. 5) ω-conotoxin CVID in dark green color. 6) ω-conotoxin CVIE in cyan color. 7) ω-conotoxin CVIF in light sea green color. 8) ω-conotoxin FVIA in blue color. 9) ω-conotoxin GVIA in comfort blue color. 10) ω-conotoxin GVIB in medium blue color. 11) ω-conotoxin GVIIA in purple color. 12) ω-conotoxin GVIIB in hot-pink color. 13) ω-conotoxin MVIIA in magenta color. 14) ω-conotoxin MVIIC in dim gray color. 15) ω-conotoxin RVIA in orange-red color. 16) ω-conotoxin TVIA in gray color. Receptor chain is highlighted with white color along with receptor-ligand surface in rosy-brown color.

Table 5: Docking result of ω-conotoxin ligands in complex with Cav 2.2 channel receptor.

Ligands	Hydrogen bonds				Hydrophobic bonds	
	Receptor residues	Ligand residues	Atoms	Distance(Å)	Receptor residues	Ligand residues
ω-conotoxin CnVIIA	GLY1326 GLN1327	SER20 SER20	OE1-N O-OG	2.55 3.26	ILE1264,VAL1273,VAL1277, PHE1274,LEU1281,LEU1416	CYS1,TYR12,ASP13, CYS14,CYS15,GLY17, CYS19,CYS26
ω-conotoxin CVIA	GLY1326 GLN1327	ARG24 ARG24	O-NH2 OD2-NH1	3.08 3.08	VAL1277,SER1280,LEU1281, VAL1284,TYR1328,PHE1361, SER1364,PHE1409,PHE1413	CYS1,LYS2,THR4, GLY5,SER12,TYR13, CYS15,THR17,CYS25
ω-conotoxin CVIB	GLN1327 GLU1319	ARG17 LYS10	OE1-NH2 OE2-NZ	2.70 2.77	ARG1322,GLY1366,GLU1367	GLY18,SER19,SER22 CYS20
ω-conotoxin CVIC	TYR1328	LYS2	OH-NZ	2.76	LEU1270,VAL1273,VAL1277, LEU1281,SER1364,THR1365, PHE1409	CYS1,SER7,MET12, THY13,CYS16,ARG22
ω-conotoxin CVID	GLY1326 GLU1319	LYS10 LYS7	O-N OE1-NZ	2.60 2.45	ASP1173,PRO1174,VAL1257, LEU1258,LEU1261,GLN1327	LYS2,SER9,LEU11, MET12,VAL24,GLY25
ω-conotoxin CVIE	GLN1327	TYR13	OE1-OH	2.77	PHE1274,VAL1277,CYS1324, TYR1328,ILE1412,LEU1416	LYS4,ALA6,SER7, ARG10,CYS20,ARG21, SER22
ω-conotoxin CVIF	GLN1327 ASP1323	ARG10 ARG21	OE1-NH2 OD1-NH2	2.64 3.03	ARG1322,PHE1361,PHE1405, PHE1409	LYS4,GLY5,ARG10, CYS16,THR17,LEU22
ω-conotoxin FVIA	GLN1327	LYS2	OE1-NZ	2.85	VAL1273,PHE1274,VAL1277, TYR1291,ILE1412,PHE1413, LEU1416	CYS1,ILE11,TYR13, CYS15,CYS16,SER19, ARG21
ω-conotoxin GVIA	GLU1334 GLU1335	TYR13 SER6	OE2-OG OE1-OG	2.55 2.66	GLY1231,ILE1249,LEU1255, LEU1258,TYR1331,LEU1354	SER7,CYS8,SER9, SER12,THR11,ARG25
ω-conotoxin GVIB	GLY1326 GLN1327	ARG22 ASN18	OD1-NH1 O-ND2	2.87 2.76	SER1166,ILE1167,PRO1174, LEU1261,GLU1321,ARG1325	SER6,CYS7,SER8,THR9, TYR11,THR20,LYS21
ω-conotoxin GVIIA	GLY1326 ARG1322	LYS23 LYS23	O-NZ O-OE	2.92 3.15	PHE1274,VAL1277,ASP1330, PHE1361,THR1365,PHE1413	ARG8,MET10,LEU19, TYR20,SER21,ASN22
ω-conotoxin GVIIB	GLN1327	LYS2	OEI-NZ	2.91	VAL1277,VAL1284,TYR1328, PHE1409,ILE1412,PHE1413	CYS1,CYS6,SER7, ARG11,THR15,SER16, LEU18
ω-conotoxin MVIIA	GLN1327	TYR13	NE2-CE2	3.15	ILE1264,LEU1270,VAL1277, TYR1328,PHE1409,LEU1416	LYS4,LEU11,MET12, CYS16,THR17,SER19, CYS20
ω-conotoxin MVIIC	GLN1327	ARG9	OE1-NE	2.86	VAL1273,PHE1274,VAL1277, LEU1285,ASP1323,CYS1324, TYR1328,THR1365,PHE1413	LYS4,GLY5,PRO7, THR11,TYR13,SER19, ARG22,LYS25
ω-conotoxin RVIA	GLN1327	TYR13	O-OH	3.25	LEU1220,LEU1224,ILE1227, LEU1281,LEU1357,PHE1361	PRO3,PRO4,CYS16, SER17,SER18,CYS19, TYR22,LYS24,LYS25
ω-conotoxin TVIA	GLN1334	ARG27	OD1-NH1	2.87	ILE1223,ILE1227,LEU1285, ILE1289,LEU1293,TYR1328, ASP1330	CYS1,TYR13,CYS16, ARG17,CYS21,TYR22

3D superimposed structures of ω-conotoxin complexes with full length Cav 2.2 channel receptor is shown in Figure 7(a). As it is clearly observed from the figure, that all complexes have strong binding affinity with the residues that reside on domain III region of receptor. In Figure 7(b), ω-conotoxins are highlighted in different color where they showed interactions with domain III region of Cav 2.2 channel receptor. Domain III is shown in rosy brown surface while the region which has binding pocket for peptides is highlighted with white color. Figure 7(c)

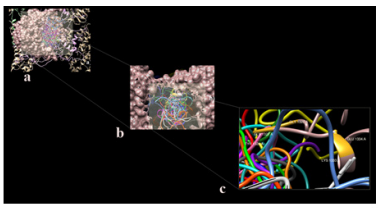

Figure 7 Complexes of ω-conotoxins with Cav 2.2 channel receptor. b) Active residues of domain III in the binding pockets are highlighted with white color of receptor with ω-conotoxins. c) ω-conotoxin CnVIIA (red color), ω-conotoxin CVIA (orange color), ω-conotoxin CVIB (yellow color), ω-conotoxin CVIC (green color), ω-conotoxin CVID (dark green color), ω-conotoxin CVIE (cyan color), ω-conotoxin CVIF (light sea green color),ω-conotoxin FVIA (blue color),ω-conotoxin GVIA (comfort blue color), ω-conotoxin GVIB (medium blue color), ω-conotoxin GVIIA (purple color), ω-conotoxin GVIIB (hot-pink color) , ω-conotoxin MVIIA (magenta color), ω-conotoxin MVIIC (dim gray color), ω-conotoxin RVIA (orange-red color) and ω-conotoxin TVIA (gray color) with the Cav 2.2 channel receptor along with the labeled active residues.

shows the active residues of domain III that lie in region between S5 and S6 helices. Six different residues i.e. GLY1326, GLN1327, TYR1328, LYS1333 and GLU1334 are highlighted with white color. According to docking results and analysis, these residues are considered as being important for blockage by ω-conotoxins. The binding residues achieved through the docking studies with Cav 2.2 channel receptor were in fact similar to already reported for the receptor with ω-conotoxins experimental data.

Energy Values

Since energy values of the complexes are directly associated to the stability of the complex, therefore lower the free energy, stronger will be the binding affinity between receptor and the ligand. The successive energy values for the ligand-receptor complex formed by each ω-conotoxin with the Cav 2.2 channel receptor is shown in Table 6 whereas Figure 8 is a graphical representation of the plotting between the ligands and their binding energies. The lowest free energy was seen for ω-conotoxin CVIB, whereas ω-conotoxin CVID and ω-conotoxin GVIA formed a complex with the Cav 2.2 channel receptor with the second lowest free energy value. ω-conotoxin CnVIIA , ω-conotoxin CVIE, ω-conotoxin CVIF, ω-conotoxin GVIIA, ω-conotoxin MVIIA and ω-conotoxin MVIIC exhibited same energy values while ω-conotoxin CVIA, ω-conotoxin CVIC, ω-conotoxin FVIA, ω-conotoxin GVIB, ω-conotoxin GVIIB and ω-conotoxin RVIA exhibited same energy values (Table 6, Figure 8). As clearly observed from the graph in Figure 8, the least free energy values lie in negative range. These energy values suggested that ω-conotoxins formed stable complexes with Cav 2.2 channel receptor.

Table 6: Binding energy values for each toxin in complex with Cav 2.2 channel receptor.

Ligands	Energy value
ω-conotoxin CnVIIA	-1.35
ω-conotoxin CVIA	-0.88
ω-conotoxin CVIB	-3.71
ω-conotoxin CVIC	-0.99
ω-conotoxin CVID	-2.35
ω-conotoxin CVIE	-1.43
ω-conotoxin CVIF	-1.91
ω-conotoxin FVIA	-0.55
ω-conotoxin GVIA	-2.19
ω-conotoxin GVIB	-0.47
ω-conotoxin GVIIA	-1.61
ω-conotoxin GVIIB	-0.38
ω-conotoxin MVIIA	-1.13
ω-conotoxin MVIIA	-1.82
ω-conotoxin RVIA	-0.38
ω-conotoxin TVIA	-1.8

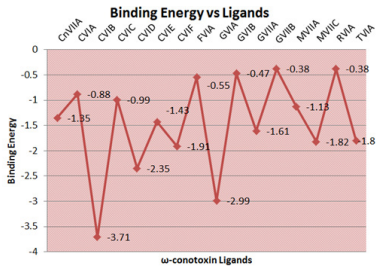

Figure 8 Graphical plot of binding energies vs. the toxin ligands.

Conclusion

The selectivity of ω-conotoxins for the α-subunit of the Cav 2.2 channel receptor had been reported as its antagonists. In this report, an in silico study was designed to analyze binding interaction of ω-conotoxins with the Cav 2.2 channel receptor in humans. After the binding interactions of both the receptor and ligands were interpreted, a comparative analysis was performed between the active site residues of receptor molecule with the toxin ligands via molecular docking method. The similarity of the computational result with the experimental data suggests the potential successful binding affinity of the toxin ligands with the receptor, as their antagonists. These results could assist to demonstrate the potential of Cav2.2 with the ω-conotoxins are valuable pharmacological tools and potentially valuable leads for treatment of neuropathic pain.

Conflict of Interest:

The authors declare that they have no conflict of interest.

Acknowledgements

The authors would like to thank for the facilities provided by their respective Departments.

References

1 Catterall WA (2000) Structure and regulation of voltage-gated Ca2+ channels. Annu Rev Cell Dev Biol 16:521–55.

2 Hofmann F, Lacinová L, Klugbauer N (1999) Voltage-dependent calcium channels: from structure to function. Rev Physiol Biochem Pharmacol 139:33–87.

3 Catterall WA, Perez-Reyes E, Snutch TP, Striessnig J (2005) International Union of Pharmacology. XLVIII. Nomenclature and structure-function relationships of voltage-gated calcium channels. Pharmacol Rev. Dec:57(4):411–25.

4 Schiano Moriello A, Luongo L, Guida F, S. Christodoulou M, Perdicchia D, Maione S, Passarella D, Di Marzo V, De Petrocellis L (2016) Chalcone Derivatives Activate and Desensitize the Transient Receptor Potential Ankyrin 1 Cation Channel, Subfamily A, Member 1 TRPA1 Ion Channel: Structure-Activity Relationships in vitro and Anti-Nociceptive and Anti-inflammatory Activity in vivo. CNS & Neurological Disorders - Drug Targets- CNS & Neurological Disorders) Oct 1 15(8):987–94.

5 Sugunan S, Nampoothiri SS, Garg T, Krishnamurthy RG (2016) Role of KCa3.1 Channels in CNS Diseases: A Concise Review. CNS Neurol Disord Drug Target 15(10):1299–305.

6 Solimini R, Rotolo MC, Pichini S, Pacifici R (2017) Neurological Disorders in Medical Use of Cannabis: An Update. CNS Neurol Disord Drug Targets 16(5):527–33.

7 Islam N, Abbas M, Rahman S (2017) Neuropathic Pain and Lung Delivery of Nanoparticulate Drugs: An Emerging Novel Therapeutic Strategy. CNS Neurol Disord Drug Targets 16(3):303–10.

8 Skaper SD (2016) Mast Cell - Glia Dialogue in Chronic Pain and Neuropathic Pain: Blood-Brain Barrier Implications. CNS Neurol Disord Drug Targets 15(9):1072–8.

9 Winquist RJ, Pan JQ, Gribkoff VK (2005) Use-dependent blockade of Cav2.2 voltage-gated calcium channels for neuropathic pain. Biochem Pharmacol. Aug 15 70(4):489–99.

10 Gomez MV, Kalapothakis E, Guatimosim C, Prado MAM (2002) Phoneutria nigriventer Venom: A Cocktail of Toxins That Affect Ion Channels. Cell Mol Neurobiol. Dec 1 22(5):579–88.

11 Lewis RJ, Garcia ML (2003) Therapeutic potential of venom peptides. Nat Rev Drug Discov. Oct 2(10):790–802.

12 Zhou Y, Niimi K, Li W, Takahashi E (2015) Effects of Cav2 2 inhibitor on hippocampal spatial short-term cognition. Integr Mol Med 2(1): 95-98

13 Saegusa H, Kurihara T, Zong S, Kazuno A, Matsuda Y, Nonaka T, Han W, Toriyama H, Tanabe T (2001) Suppression of inflammatory and neuropathic pain symptoms in mice lacking the N-type Ca2+ channel. The EMBO journal. 20(10) 2349–2356.

14 Zhang Y (2008) I-TASSER server for protein 3D structure prediction. BMC bioinformatics. 9(1):40.

15 Lewis RJ, Nielsen KJ, Craik DJ, Loughnan ML, Adams DA, Sharpe IA, Luchian T, Adams DJ, Bond T, Thomas L, Jones A, Matheson JL, Drinkwater R, Andrews PR, Alewood PF (2000) Novel omega-conotoxins from Conus catus discriminate among neuronal calcium channel subtypes. J Biol Chem. Nov 10 275(45):35335–44.

16 Stocker JW, Nadasdi L, Aldrich RW, Tsien RW (1997) Preferential Interaction of ω-Conotoxins with Inactivated N-type Ca2+ Channels. J Neurosci. May 1 17(9):3002–13.

17 Feng Z-P, Hamid J, Doering C, Bosey GM, Snutch TP, Zamponi GW (2001) Residue Gly1326 of the N-type Calcium Channel α1B Subunit Controls Reversibility of ω-Conotoxin GVIA and MVIIA Block. J Biol Chem. May 11 276(19):15728–35.

18 Lewis RJ, Dutertre S, Vetter I, Christie MJ (2012) Conus venom peptide pharmacology. Pharmacol Rev Apr 64(2):259–98.

19 Olivera BM (2006) Conus peptides: biodiversity-based discovery and exogenomics. J Biol Chem. Oct 20 281(42):31173–7.

20 Norton RS, Pallaghy PK (1998) The cystine knot structure of ion channel toxins and related polypeptides. Toxicon. Nov 36(11):1573–83.

21 Berman HM, Westbrook J, Feng Z, Gilliland G, Bhat TN, Weissig H, Shindyalov IN, Bourne PE (2000) The Protein Data Bank. Nucleic Acids Res. Jan 1;28(1):235–42.

22 Simossis VA, Heringa J (2005) PRALINE: a multiple sequence alignment toolbox that integrates homology-extended and secondary structure information. Nucleic Acids Research. Jul 1 33(Web Server issue):W289.

23 Nielsen KJ, Adams D, Thomas L, Bond T, Alewood PF, Craik DJ, Lewis RJ (1999) Structure-activity relationships of $ømega$-conotoxins MVIIA, MVIIC and 14 loop splice hybrids at N and P/Q-type calcium channels. Journal of molecular biology. 289(5):1405–1421.

24 Skalicky JJ, Metzler WJ, Ciesla DJ, Galdes A, Pardi A. Solution structure of the calcium channel antagonist omega-conotoxin GVIA (1993) Protein Science : A Publication of the Protein Society. Oct 2(10):1591.

25 Lew MJ, Flinn JP, Pallaghy PK, Murphy R, Whorlow SL, Wright CE, Norton RS, Angus JA (1997) Structure-function relationships of omega-conotoxin GVIA. Synthesis, structure, calcium channel binding, and functional assay of alanine-substituted analogues. J Biol Chem. May 2 272(18):12014–23.

26 Sato K , Park Ng, Kohno T, Maeda T, Kim J I, R Kato, Takahashi M (1993) Role of basic residues for the binding of omega-conotoxin GVIA to N-type calcium channels. Biochem Biophys Res Commun. Aug 1 194(3):1292–6.

27 Morris GM, Huey R, Lindstrom W, Sanner MF, Belew RK, Goodsell DS, Olson AJ (2009) AutoDock4 and AutoDockTools4: Automated Docking with Selective Receptor Flexibility. J Comput Chem. Dec 30(16):2785–91.

28 Pettersen EF, Goddard TD, Huang CC, Couch GS, Greenblatt DM, Meng EC, Ferrin TE(2004) UCSF Chimera--a visualization system for exploratory research and analysis. J Comput Chem. Oct 25(13):1605–12.

29 Wallace AC, Laskowski RA, Thornton JM (1995) LIGPLOT: a program to generate schematic diagrams of protein-ligand interactions. Protein Eng. Feb 8(2):127–34.